

# Analysis of Pointing Loss Effects in Deep Space Optical Links

Lorenzo Valentini, Alberto Faedi, Enrico Paolini, Marco Chiani  
CNIT, DEI, University of Bologna, Cesena, Italy  
Email: {lorenzo.valentini13, e.paolini, marco.chiani}@unibo.it

**Abstract**—Owing to the extremely narrow beams, a main issue in optical deep space communications is represented by miss-pointing errors, which may severely degrade the system performance and availability. In this paper, we address pointing losses in the case in which both the receiver and the transmitter are affected by angular errors. Pointing losses are evaluated through two approaches. The first approach is deterministic and only requires knowledge of a maximum angular error. The second approach requires knowledge of the angular error statistical distribution and tackles the problem from an outage probability viewpoint. These tools are then applied to analyze the impact of pointing losses in deep space optical links in which both terminals suffer from miss-pointing effects. The antenna gains are first optimized to maximize the effective system gain. The optimum antenna gains are then applied to evaluate maximum achievable ranges and to perform link design by means of optical link budgets.

**Index Terms**—Deep space communications, free-space optical communications, pointing loss, satellite relaying, serially concatenated pulse position modulation.

## I. INTRODUCTION

Free space optical links offer an attractive alternative in wireless communications, for data transmission at very high rates over long distances. Licence-free spectrum and low mass and power requirements are features fostering the use of optical frequencies in several application domains [1], [2], including high-speed transportation, unmanned aerial vehicles, building-to-building communications, satellite and deep space communications [3]. The raising demand for telemetry (TM) data from space and the growing volumes of such data, in particular, are contributing to the increasing interest for optical bands in space communications, with the expectation to boost data rates by two orders of magnitude over conventional radio-frequency (RF) links [1], [4].

In the recent past, several space missions have exploited optical frequencies. In 2001, the European Space Agency (ESA) implemented and tested an inter-satellite laser link within the Semiconductor-laser Intersatellite Link EXperiment (SILEX) mission. In 2009, the National Aeronautics and Space Administration (NASA) Mars Laser Communications Demonstration (MLCD) proved the feasibility of deep space optical communications; moreover, in 2013, the NASA Lunar Laser Communications Demonstration (LLCD) mission demonstrated high-rate laser communications from a small terminal at lunar distances. In 2014, the NASA Optical Payload for Lasercomm Science (OPALS) mission aimed at demonstrating optical communications between the International

Space Station (ISS) and Earth ground stations. In 2016 and 2019, the ESA European Data Relay Satellite (EDRS) mission sent into geosynchronous equatorial orbit two satellites with the goal of providing near global coverage for satellites in low-Earth orbit, exploiting optical links.

Although the above-mentioned missions have confirmed that optical frequencies can achieve higher data rates with lower size and mass with respect to the RF case, their use in space links also poses several challenges. In this respect, main issues are represented by pointing errors, solar conjunctions, and atmospheric effects [5]–[8]. Even in an inter-satellite scenario, where atmospheric effects are absent, the pointing losses alone can frustrate the benefits offered by the optical frequencies. Hence, several studies have been conducted to model and analyze these losses [1], [9]–[12]. The extremely narrow optical beams, essential in deep space communications to maximize the received power, pose very tight requirements in terms of pointing accuracy. As a consequence, the miss-pointing losses between the transmit and the receive antennas cannot be neglected even in presence of a very accurate point-ahead calculation, due to mechanical noise generated by the vibrations and the satellite motions [13].

Most available studies on pointing effects assume that only one antenna is affected by angular errors [5]. For example, when one edge of the communication link is on ground, a very precise ground pointing can be assumed and, therefore, it is usual to consider the angular noise only on the spacecraft. In case of space-to-space links, however, pointing effects should be carefully considered at both edges of the link. A particularly interesting situation where this problem arises is represented by “two-hop” deep space communication architectures, featuring a first optical link between a deep space probe and a relay orbiting the Earth (to avoid atmospheric impairments), and a second link between the relay and the Earth using, e.g., a classical RF frequency. Therefore, in this paper we investigate approaches to address the miss-pointing losses in situations where both terminals are affected by angular noise. The concept of *effective system gain* is introduced and the effect of pointing losses is investigated in terms of maximum achievable ranges and of deep space optical link budgets.

This paper is organized as follows. Section II addresses angular error distributions and pointing loss models. Section III describes two approaches to pointing losses, the first based on a maximum angular error and the second on the angular error statistic. Section IV addresses gain optimization, with

application to maximum achievable ranges and optical link budgeting. Conclusions are drawn in Section V.

## II. SYSTEM MODEL

In this section we introduce our assumptions as well as the pointing error descriptions over free space communication links. We also report three pointing loss models that can be used according to the antenna features [11], [13]. The combination of these descriptions allows analyzing and addressing the communication limits due to pointing errors.

### A. Angular Error Distribution

Pointing in a three-dimensional space is affected by both azimuth and elevation angular errors. In this paper we assume that these two errors are independent and identically distributed (i.i.d.) and Gaussian distributed with zero-mean. Therefore, the resulting random angular error  $\theta$ , the angle between the line of sight (LOS) and the pointing direction, is Rayleigh distributed as [13], [14]

$$f_{\theta}(\theta) = \frac{\theta}{\sigma_{\theta}^2} e^{-\theta^2/2\sigma_{\theta}^2}, \quad \theta \geq 0 \quad (1)$$

where  $\sigma_{\theta}$  is the main angular noise parameter, hereafter referred to as the *pointing accuracy*. Another model, sometimes used in the literature, assumes the azimuth and elevation angular errors as independent and Gaussian, but with a non-zero mean. This yields an angular error that is Rician-distributed according to [2], [5]

$$f_{\theta}(\theta) = \frac{\theta}{\sigma_{\theta}^2} e^{-(\theta^2 + \eta^2)/2\sigma_{\theta}^2} I_0\left(\frac{\theta\eta}{\sigma_{\theta}^2}\right), \quad \theta \geq 0 \quad (2)$$

where  $I_0(\cdot)$  is the modified Bessel function of the first kind of order 0, and  $\eta$  is the bias error angle from the center.

### B. Pointing Loss Models

The pointing losses are described by the radiation pattern of the antenna. In fact, they can be seen as a ‘‘correction factor’’ accounting for the gain  $G$  being set equal to its maximum value  $G_{\max}$ . Hence, in order to analyze these losses, a description of the antenna gain, parameterized by the angular miss-pointing along the LOS direction, is required. In the following we summarize the models used in this paper, where  $G$  is the linear-domain antenna gain and  $\theta$  is the angular miss-pointing error. In case of Gaussian beam, the pointing losses are given by [13]

$$L_p(\theta) = e^{-G\theta^2}. \quad (3)$$

In case of circular aperture, the pointing losses are instead given by [13], [15]

$$L_p(\theta) = \left(\frac{2J_1(\sqrt{G}\theta)}{\sqrt{G}\theta}\right)^2 \quad (4)$$

where  $J_1(\cdot)$  is the Bessel function of the first kind of order 1. This latter model can be well-approximated, for small angular

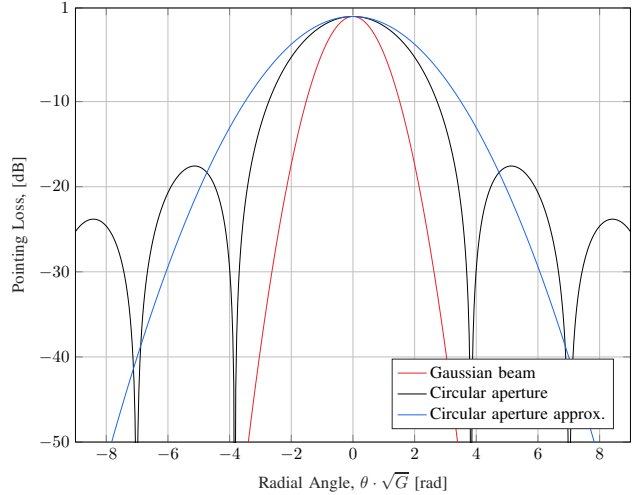


Fig. 1. Comparison between different pointing loss models.

error  $\theta$ , as [16]

$$L_p(\theta) = \left(\frac{2J_1(\sqrt{G}\theta)}{\sqrt{G}\theta}\right)^2 \approx e^{-\alpha G\theta^2} \quad (5)$$

where  $\alpha = 0.188$ . Fig. 1 illustrates the pointing losses computed according to the above models.

## III. POINTING LOSSES

In this section we address two approaches to quantify pointing losses. The first approach treats the angular error as a *deterministic parameter* (usually regarded as the maximum angular error); the second one considers the angular error as a *random variable*, which allows formulating the problem in terms of an outage probability.

### A. Deterministic Approach

The deterministic approach consists of simply taking a maximum angular error  $\theta_{\max}$  (based on the available information about the tracking system) and of quantifying the pointing loss by employing one of the above-presented models, using the numerical value of  $\theta_{\max}$ . This method is useful in case no a priori knowledge is available about the statistical distribution of the angular error. For example, using a Gaussian beam model, for given  $\theta_{\max}$  we compute the maximum pointing loss to be included in the power budget as

$$L_{p,\max} = e^{-G\theta_{\max}^2}. \quad (6)$$

This procedure is simple but provides no information about the probability that the actual pointing loss  $L_p$  exceeds the value  $L_{p,\max}$  during its random fluctuations. In other words, it is unable to capture the concept of outage.

### B. Outage Probability Approach

In contrast with the deterministic approach, we propose a statistical approach introducing a pointing outage probability

defined as

$$P_{\text{out}} = \mathbb{P}\{A_p[\text{dB}] > A_p^*[\text{dB}]\} \quad (7)$$

where  $A_p[\text{dB}] = -L_p[\text{dB}]$  and  $A_p^*[\text{dB}]$  is the margin against the pointing attenuation to be included in the link budget. Hence, we define the outage probability as the probability that the pointing loss exceeds the maximum value we can compensate with the employed margin  $A_p^*[\text{dB}]$ .

In case of a link between two antennas, both affected by mechanical noise, it is necessary to consider the pointing losses introduced by each of them. In this situation, we can write

$$P_{\text{out}} = \mathbb{P}\{A_{p,t}[\text{dB}] + A_{p,r}[\text{dB}] > A_p^*[\text{dB}]\} \quad (8)$$

where the subscripts ‘ $t$ ’ and ‘ $r$ ’ refer to the transmitter and the receiver, respectively. Hence, to compute the outage probability both error distributions and antenna gain radiation pattern are required.

In case both radiation patterns follow the Gaussian beam model and the two angular errors are independent and Rayleigh distributed with parameters  $\sigma_{\theta,t}$  and  $\sigma_{\theta,r}$ , we obtain

$$P_{\text{out}} = \mathbb{P}\{G_t\theta_t^2 + G_r\theta_r^2 > K\} \quad (9)$$

where  $K = \frac{\ln(10)}{10} A_p^*[\text{dB}]$ . Substituting  $y_r = \theta_r^2$  and  $y_t = \theta_t^2$ , we obtain two independent exponential random variables with mean values  $2\sigma_{\theta,t}^2$  and  $2\sigma_{\theta,r}^2$ , yielding

$$\begin{aligned} P_{\text{out}} &= 1 - \int_0^{K/G_r} \int_0^{\frac{K-G_r y_r}{G_t}} \frac{1}{4\sigma_{\theta,t}^2\sigma_{\theta,r}^2} e^{-\left[\frac{y_t}{2\sigma_{\theta,t}^2} + \frac{y_r}{2\sigma_{\theta,r}^2}\right]} dy_t dy_r \\ &= \frac{G_t\sigma_{\theta,t}^2 e^{-K/(2\sigma_{\theta,t}^2 G_t)}}{G_t\sigma_{\theta,t}^2 - G_r\sigma_{\theta,r}^2} + \frac{G_r\sigma_{\theta,r}^2 e^{-K/(2\sigma_{\theta,r}^2 G_r)}}{G_r\sigma_{\theta,r}^2 - G_t\sigma_{\theta,t}^2}. \end{aligned} \quad (10)$$

For given  $P_{\text{out}}$ , antenna gains, and pointing accuracy parameters, (10) allows obtaining  $A_p^*$  (through  $K$ ) numerically. In the particular case  $G_t = G_r = G$  and  $\sigma_{\theta,t} = \sigma_{\theta,r} = \sigma_{\theta}$ , the outage probability becomes

$$P_{\text{out}} = \left(1 + \frac{K}{2\sigma_{\theta}^2 G}\right) e^{-K/2\sigma_{\theta}^2 G}. \quad (11)$$

Very similar results are obtained, by introducing the parameter  $\alpha$ , for the circular aperture model through the approximation described in (5). This approximation is tight when pointing losses accounted for in the link budget  $A_p^*$  are small (small angular error) as depicted in Fig. 1. We simply have

$$P_{\text{out}} = \frac{G_t\sigma_{\theta,t}^2 e^{-K/(2\sigma_{\theta,t}^2 \alpha G_t)}}{G_t\sigma_{\theta,t}^2 - G_r\sigma_{\theta,r}^2} + \frac{G_r\sigma_{\theta,r}^2 e^{-K/(2\sigma_{\theta,r}^2 \alpha G_r)}}{G_r\sigma_{\theta,r}^2 - G_t\sigma_{\theta,t}^2}. \quad (12)$$

Different models or error distributions may require numerical evaluation. Also note that, in case only one antenna (either on the transmit or on the receive side) is affected by miss-pointing errors, we can ‘‘artificially’’ obtain the outage probability by simply letting either  $G_r$  or  $G_t$  be null. For example, under a Gaussian beam model and letting miss-pointing error affect the receiver only, setting  $G_t = 0$  and

$G_r = G$  in (10), we obtain

$$P_{\text{out}} = e^{-K/2\sigma_{\theta}^2 G}. \quad (13)$$

This is useful when one of the two losses dominates the other or when the effect of pointing errors on one side is negligible.

#### IV. APPLICATION TO DEEP SPACE OPTICAL LINKS

Hereafter we focus on a deep space optical TM link with photon counting receiver and Poisson channel model [17], [18]. The considered coding and modulation scheme is the serially concatenated pulse-position modulation (SCPPM) one, recommended by the Consultative Committee for Space Data Systems (CCSDS) for the Coding and Synchronization Sublayer of deep space optical TM [19], [20]. The encoder features a serial concatenation of a convolutional encoder, an interleaver, an accumulator, and a pulse position modulator. The advantage of SCPPM lays on the possibility to iteratively decode the received symbols achieving near-capacity performance [18].<sup>1</sup> The PPM is often employed in deep space links, where peak and average power constraints are typical [24]–[26]. The output of the PPM modulator is a symbol composed of  $M = 2^m$  slots, of which only one is pulsed; the position of the laser pulse in a symbol is given by the configuration of the corresponding  $m = \log_2 M$  input bits. Over a Poisson channel, the receiver observes a number  $k$  of photons in each slot distributed according to

$$\begin{aligned} \mathbb{P}\{k \mid \text{slot pulsed}\} &= \frac{(n_s + n_b)^k}{k!} e^{-(n_s + n_b)} \\ \mathbb{P}\{k \mid \text{slot not pulsed}\} &= \frac{n_b^k}{k!} e^{-n_b} \end{aligned} \quad (14)$$

where  $n_s$  is the mean number of signal photons per slot, and  $n_b$  is the mean number of noise photons per slot.

##### A. Antenna Gain Optimization

Regardless of the approach used to estimate the pointing losses and the adopted model, we can define an ‘‘effective system gain’’ as

$$G_{\text{eff}} = (G_t L_{p,t}) (G_r L_{p,r}) \quad (15)$$

i.e., as the product of the transmit and receive antenna gains, each multiplied by the corresponding pointing loss. Looking at the effective system gain reveals the existence of an optimal value for the antenna gains, beyond which the overall system performance degrades instead of improving. Considering a situation where the transmitter and the receiver are equipped with the same antennas, the effective system gain, expressed in dB, assumes the form

$$G_{\text{eff}} [\text{dB}] = 2G [\text{dB}] - A_{p,\text{tot}} [\text{dB}] \quad (16)$$

where  $A_{p,\text{tot}}[\text{dB}]$  incorporates the total pointing losses. Sticking for simplicity to the case in which both antennas exhibit the same pointing accuracy parameter, defined either by  $\sigma_{\theta}$

<sup>1</sup>We point out the existence of other competitive coding schemes for pulse-position modulation (PPM) optical communications, such as binary LDPC codes [21], [22] and nonbinary LDPC codes [23].

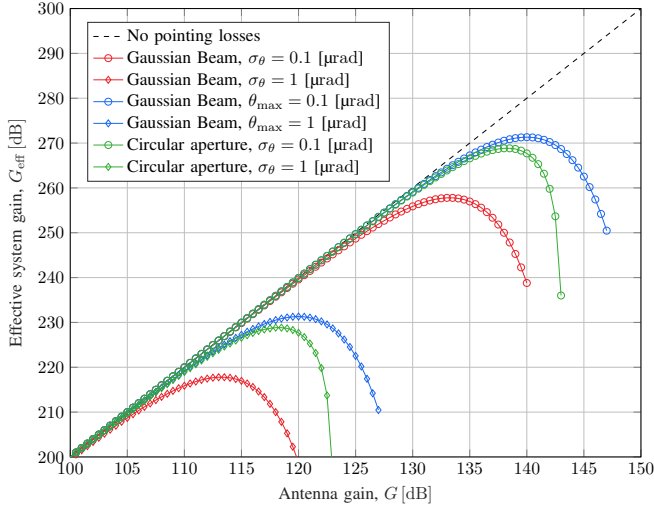


Fig. 2. Effective system gain versus the antenna gain. Deterministic and probabilistic approach to the pointing losses; different values of the pointing accuracy parameters; Gaussian beam and circular aperture models.

or by  $\theta_{\max}$  depending on the employed approach, we can numerically find the total pointing attenuation  $A_{p,\text{tot}}[\text{dB}]$  (and therefore the numerical value of  $G_{\text{eff}}[\text{dB}]$ ) for any given gain  $G[\text{dB}]$ .

An example is shown in Fig. 2 for different values of the pointing accuracy parameter ( $\sigma_\theta$  or  $\theta_{\max}$ ) and different pointing loss models (Gaussian beam or circular aperture). In case the probabilistic approach is used, the outage probability is set to  $P_{\text{out}} = 5\%$ . The red and green curves correspond to the probabilistic approach for the Gaussian beam and circular aperture models, respectively; the blue curves refer to the deterministic approach in the case of Gaussian beam.

**Remark.** The optimal gain in the Gaussian beam case, when the approach based on  $\theta_{\max}$  is used, can be easily derived as

$$G_{\text{opt}} = \frac{1}{\theta_{\max}^2}. \quad (17)$$

### B. Maximum Achievable Range

The effective gain defined above can be used to analyze the maximum achievable range in optical deep space links in which both antennas are affected by miss-pointing errors. A scenario where this analysis is particularly relevant is represented by an optical link between a deep space probe and a second spacecraft orbiting Earth and acting as a relay towards the ground station.

The analysis is carried out for a wavelength  $\lambda = 1064 \text{ nm}$ . We choose the SCPPM parameters to minimize the smallest received power such that  $P_e \leq P_e^*$ , where  $P_e$  is the block error probability and  $P_e^*$  is its target value. Accordingly, we set the PPM slot time as  $T_s = 256 \text{ ns}$ , the convolutional code rate as  $R = 1/3$ , and the guard time between two adjacent PPM symbols, following the CCSDS recommendation, to  $\alpha_{\text{gt}} = 25\%$ . More specifically, this constraint imposes  $M/4$  idle slots between any two adjacent PPM symbols to guarantee the laser

recharge. Moreover, we consider an efficiency equal to  $-5 \text{ dB}$  for both the transmit and the receive antennas, a supplementary detection and implementation loss equal to  $-4 \text{ dB}$ , a mean value of the background noise flux  $n_b = 1.21 \cdot 10^7 \text{ phe/ns}$ , and  $P_e^* = 10^{-4}$  [10]. Concerning pointing losses, we take  $P_{\text{out}} = 5\%$  when applying the probabilistic approach and, for both the deterministic approach and the probabilistic one, we adopt the Gaussian beam model (worst case). Furthermore, we assume that the transmit and receive antennas are equal to each other in terms of both gain and pointing accuracy parameter  $\sigma_\theta$  or  $\theta_{\max}$ . Applying the analysis described in Section IV-A, we design the antenna gains to achieve the maximum effective gain. Lastly, in compliance with International Telecommunication Union (ITU) recommendations [12] the link margin is set to  $3 \text{ dB}$  and the average transmit power to  $5 \text{ W}$ . No atmospheric attenuation is considered since, as previously mentioned, the receiver is assumed to be a relay orbiting outside the Earth atmosphere.

Table I and Table II show the maximum achievable ranges in astronomic unit (AU) (where  $1 \text{ AU} = 149,597,871 \text{ Km}$ ) for both pointing loss approaches. In both tables, each column refers to one specific PPM order  $M$  (the number of slots in one PPM symbol), which influences the minimum received power such that  $P_e \leq P_e^*$ , the transmit peak power, and the information data rate. On the other hand, each row refers to a specific value of the pointing accuracy parameter.

The obtained results reveal how the pointing accuracy is a very critical parameter in the optical link design. As  $\sigma_\theta$  or  $\theta_{\max}$  varies, we observe large achievable rate variations for the same PPM order, target performance, and information data rate. This is related to the impossibility to achieve unbounded gains when pointing losses are included in the model, especially if they are included both in the transmitter and in the receiver. We can also compare the results one would obtain without including pointing losses in the analysis, to remark the importance of a correct evaluation pointing losses in deep space inter satellite optical links. Considering, for example, the case  $M = 256$ , using the deterministic method with  $\theta_{\max} = 0.35 \text{ urad}$ , using the same antenna gains but neglecting pointing losses, the maximum achievable range would be  $11.63 \text{ AU}$ , almost three times larger than the value  $4.397 \text{ AU}$  reported in Table II.

### C. Link Budget

Finally we provide an example of TM optical link budget. In particular, we consider a deep space probe orbiting Mars and communicating with a relay orbiting the Earth. There are three fundamental steps in the link budget procedure. Firstly, the optical gain and the pointing losses are derived, through the procedure described in Sec. IV-A, from the pointing requirements and the wavelength. Hereafter we use the deterministic approach with  $\theta_{\max} = 35 \text{ urad}$  and we assume the same gain and the same pointing accuracy parameter for both the transmit and receive antennas. This results in an optimal gain of  $129 \text{ dB}$  when the Gaussian beam is considered. Next, through the optical link equation we compute the received average number

TABLE I  
 MAXIMUM ACHIEVABLE RANGES, IN AU, WITH A GIVEN PPM ORDER AND A SPECIFIED  $\sigma_\theta$ . RESULTS FOUND USING GAUSSIAN BEAM MODEL,  
 $R = 1/3$ ,  $T_s = 256$  ns,  $n_b = 1.21 \cdot 10^7$  phe/s,  $P_{av} = 5$  W,  $P_{out} = 5\%$ ,  $\lambda = 1064$  nm, LINK MARGIN 3 dB.

$\sigma_\theta$ [μrad]	PPM Order / Peak Laser Power [W]						
	256 / 1600	128 / 800	64 / 400	32 / 200	16 / 100	8 / 50	4 / 25
1.00	0.113	0.084	0.062	0.046	0.034	0.025	0.019
0.50	0.453	0.336	0.249	0.184	0.136	0.101	0.075
0.35	0.924	0.684	0.507	0.375	0.277	0.206	0.152
0.20	2.836	2.100	1.555	1.151	0.851	0.631	0.467
0.15	5.037	3.730	2.762	2.045	1.512	1.121	0.830
0.10	11.342	8.398	6.218	4.605	3.406	2.525	1.869
0.05	45.350	33.580	24.864	18.411	13.617	10.094	7.474
Data Rate [kbps]	32.33	56.58	97.00	161.66	258.66	387.99	517.32

TABLE II  
 MAXIMUM ACHIEVABLE RANGES, IN AU, WITH A GIVEN PPM ORDER AND A SPECIFIED  $\theta_{max}$ . RESULTS FOUND USING GAUSSIAN BEAM MODEL,  
 $R = 1/3$ ,  $T_s = 256$  ns,  $n_b = 1.21 \cdot 10^7$  phe/s,  $P_{av} = 5$  W,  $P_{out} = 5\%$ ,  $\lambda = 1064$  nm, LINK MARGIN 3 dB.

$\theta_{max}$ [μrad]	PPM Order / Peak Laser Power [W]						
	256 / 1600	128 / 800	64 / 400	32 / 200	16 / 100	8 / 50	4 / 25
1.00	0.539	0.399	0.295	0.219	0.162	0.120	0.089
0.50	2.155	1.596	1.182	0.875	0.647	0.480	0.355
0.35	4.397	3.256	2.411	1.785	1.320	0.979	0.725
0.20	13.470	9.974	7.385	5.468	4.044	2.998	2.220
0.15	23.807	17.628	13.053	9.665	7.148	5.299	3.924
0.10	53.880	39.896	29.541	21.874	16.178	11.993	8.880
Data Rate [kbps]	32.33	56.58	97.00	161.66	258.66	387.99	517.32

of signal photons per second,  $n_s$ , as [1], [9]–[11]

$$n_s = P_{av} G_t \eta_t \left( \frac{\lambda}{4\pi r} \right)^2 G_r \eta_r L_{p,tot} L_{other} \frac{\lambda}{hc} \quad (18)$$

where  $G_t$  and  $G_r$  are the transmit and receive antenna gains,  $\eta_t$  and  $\eta_r$  are their corresponding efficiencies,  $\lambda$  is the laser wavelength,  $h$  and  $c$  are the Planck's constant and the speed of light,  $r$  is the distance between the antennas,  $P_{av}$  is the average laser power,  $L_{p,tot}$  are the pointing losses, and  $L_{other}$  are extra losses (detection and implementation ones). Finally, we find a suitable configuration of the SCPPM parameters  $M$ ,  $R$ , and  $T_s$ . The goal is to have

$$LM [dB] = n_s [dB] - n_s^{\min} [dB]. \quad (19)$$

where  $LM [dB]$  is the requested link margin and  $n_s^{\min} = n_s^{\min}(M, R, T_s, n_b)$  is the value of  $n_s$  such that  $P_e = P_e^*$ . The information data rate is then given by

$$B_r = \frac{15120 R - 34}{MT_s (15120 / \log_2 M) \alpha_{gt}} \quad (20)$$

where  $\alpha_{gt}$  is the guard time, 15120 is the SCPPM codeword length, and 34 is the number of cyclic redundancy check (CRC) and termination bits.

Table III summarizes the parameters and the resulting data. The maximum Mars-Earth distance is considered, to provide a worst case analysis. From (18),  $n_s = -33.67$  dB phe/ns is obtained. In order to guarantee a link margin compliant with the ITU recommendation [12], a PPM order  $M = 64$ , a convolutional code rate  $R = 1/3$ , and a  $T_s = 256$  ns have been selected, leading to  $n_s^{\min} = -35.76$  dB phe/s, information

data rate of 100 kbps and a link margin of 2.09 dB. Again, no atmospheric losses have been considered as the receiver is assumed outside the Earth atmosphere. A similar analysis was carried out assuming a deep space spacecraft orbiting Venus. Owing to the smaller worst-case distance, equal to 1.74 AU, in the Venus case it is possible to choose a PPM order  $M = 64$ , a code rate  $R = 1/3$ , and a slot time  $T_s = 64$  ns to achieve a data rate of 390 kbps, with a link margin of 2.17 dB.

Considering no pointing losses in the link budget and using the same input data, the modulation parameters would be mistakenly chosen as  $M = 64$ ,  $R = 1/3$ , and  $T_s = 16$  ns leading, in the Mars case, to  $B_r = 1.55$  Mbps with an expected link margin of 3.07 dB. However, due to miss-pointing, the actual link margin would be  $-5.38$  dB. This highlights the importance of an accurate miss-pointing errors estimation and the fundamental role played by antenna gain optimization.

## V. CONCLUSION

In this paper, we investigated the effect of pointing losses on optical links in a general scenario where both the transmit and receive antennas are affected by mechanical noise. We defined two approaches which differ in terms of knowledge of the angular error statistics. As opposed to the deterministic approach, the probabilistic one formulates the problem in terms of an outage probability. The developed framework allows evaluating the pointing losses even in presence of different error distributions and radiation patterns, for example, due to an asymmetric design of the transmitter and the receiver. Results have been presented in terms of effective system

TABLE III

EXAMPLE OF MARS TM OPTICAL LINK BUDGET WITH POINTING LOSSES ON BOTH THE TRANSMITTER AND THE RECEIVER. MAXIMUM EFFECTIVE SYSTEM GAIN.

Link Parameter	dB		Units
<i>Signaling and Fixed Parameter</i>			
PPM Order	64		
Convolutional Code Rate	1/3		
Slot Time	256		ns
Guard Time	25		%
Mean Noise Flux	-19.17	1.21e-02	phe/ns
Mean Noise Flux per slot		3.10	phe/slot
$\theta_{max}$ , Gaussian Beam		0.35	$\mu$ rad
<i>Laser Transmitter</i>			
Average Laser Power	6.99	5.00	W
Peak Laser Power	26.02	400	W
Wavelength		1064	nm
<i>Deep Space Orbiter</i>			
Far-Field Antenna Gain	129.00		
Transmitter Efficiency	-5.00		
<i>Range</i>			
Space Loss	-373.49	2.68	AU
<i>Near Earth Orbiter</i>			
Receiver Gain	129.00		
Receiver Efficiency	-5.00		
<i>Other</i>			
Detection/Implementation Losses	-4.00		
Pointing Loss	-8.45		
<i>Link Performance</i>			
Average Received Power	-130.96		W
Average Received Photon Flux	-33.67	4.30e-04	phe/ns
Minimum Average Received Power	-133.05		W
Minimum Average Received Photon Flux	-35.76	2.65e-04	phe/ns
Link Margin	2.09		
FER target		9.00e-05	
Information Data Rate		0.10	Mbps

gain optimization, maximum achievable ranges in deep space applications, and inter-planetary optical link budgets.

#### ACKNOWLEDGMENT

This work was supported in part by ESA/ESTEC under contract 4000132053/20/NL/FE.

#### REFERENCES

- [1] H. Hemmati, A. Biswas, and I. B. Djordjevic, "Deep-space optical communications: Future perspectives and applications," *Proc. IEEE*, vol. 99, no. 11, pp. 2020–2039, 2011.
- [2] H. Kaushal and G. Kaddoum, "Optical communication in space: Challenges and mitigation techniques," *IEEE Commun. Surveys Tuts.*, vol. 19, no. 1, pp. 57–96, 2017.
- [3] V. W. Chan, "Free-space optical communications," *J. Lightw. Technol.*, vol. 24, no. 12, pp. 4750–4762, 2006.
- [4] J. Layland and L. Rauch, *The evolution of technology in the deep space network: A history of the advanced systems program*. NASA/JPL, 1995.
- [5] V. Vilmrotter, "The effects of pointing errors on the performance of optical communications systems," *TDA Prog. Rep. 42*, vol. 63, 1981.

- [6] X. Zhu and J. M. Kahn, "Free-space optical communication through atmospheric turbulence channels," *IEEE Trans. Commun.*, vol. 50, no. 8, pp. 1293–1300, 2002.
- [7] A. A. Farid and S. Hranilovic, "Outage capacity optimization for free-space optical links with pointing errors," *J. Lightw. Technol.*, vol. 25, no. 7, pp. 1702–1710, 2007.
- [8] G. Xu and M. Zeng, "Solar scintillation effect for optical waves propagating through gamma-gamma coronal turbulence channels," *IEEE Photon. J.*, vol. 11, no. 4, pp. 1–15, 2019.
- [9] N. K. Lyras, A. D. Panagopoulos, and P.-D. Arapoglou, "Deep-space optical communication link engineering: Sensitivity analysis," *IEEE Aerosp. Electron. Syst. Mag.*, vol. 34, no. 11, pp. 8–19, 2019.
- [10] A. Biswas, H. Hemmati, S. Piazzolla, B. Moision, K. Birnbaum, and K. Quirk, "Deep-space optical terminals (DOT) systems engineering," *IPN Prog. Rep.*, vol. 42, p. 183, 2010.
- [11] A. Biswas and S. Piazzolla, "Deep-space optical communications down-link budget from Mars: System parameters," *IPN Prog. Rep.*, vol. 42, no. 154, 2003.
- [12] "Technical and operational characteristics of interplanetary and deep-space systems operating in the space-to-Earth direction around 283 Thz," Rec. ITU-R SA.1742, 2006.
- [13] C.-C. Chen and C. S. Gardner, "Impact of random pointing and tracking errors on the design of coherent and incoherent optical intersatellite communication links," *IEEE Trans. Commun.*, vol. 37, no. 3, pp. 252–260, 1989.
- [14] J. Barry and G. Mecherle, "Beam pointing error as a significant design parameter for satellite-borne, free-space optical communication systems," *Optical Engineering*, vol. 24, no. 6, p. 241049, 1985.
- [15] S. J. Orfanidis, "Electromagnetic waves and antennas, 2008." [Online]. Available: available: <http://www.ece.rutgers.edu/orfanidi/ewa>
- [16] G. Maral, M. Bousquet, and Z. Sun, *Satellite Communications Systems: Systems, Techniques and Technology*. John Wiley & Sons, 2020.
- [17] V. Vilmrotter, A. Biswas, W. Farr, D. Fort, and E. Sigman, "Design and analysis of a first-generation optical pulse-position modulation receiver," *The Interplanetary Netw. Prog. Rep. 42-148*, pp. 1–20, 2002.
- [18] B. Moision and J. Hamkins, "Deep-space optical communications down-link budget: modulation and coding," *IPN Prog. Rep.*, vol. 42, no. 154, pp. 1–28, 2003.
- [19] —, "Coded modulation for the deep-space optical channel: serially concatenated pulse-position modulation," *IPN Prog. Rep.*, vol. 42, no. 161, pp. 1–26, 2005.
- [20] C. C. for Space Data Systems, "Recommendation for space data system standards, optical communications coding and synchronization," *CCSDS 142.0-B-1*, vol. Blue Book, August 2019.
- [21] Y. Tan, J.-z. Guo, Y. Ai, W. Liu, and Y.-J. Fei, "A coded modulation scheme for deep-space optical communications," *IEEE Photon. Technol. Lett.*, vol. 20, no. 5, pp. 372–374, 2008.
- [22] H. Zhou, M. Jiang, C. Zhao, and J. Wang, "Optimization of protograph-based LDPC coded BICM-ID for the Poisson PPM channel," *IEEE Commun. Lett.*, vol. 17, no. 12, pp. 2344–2347, 2013.
- [23] B. Matuz, E. Paolini, F. Zabini, and G. Liva, "Non-binary LDPC code design for the Poisson PPM channel," *IEEE Trans. Commun.*, vol. 65, no. 11, pp. 4600–4611, 2017.
- [24] R. Lipes, "Pulse-position-modulation coding as near-optimum utilization of photon counting channel with bandwidth and power constraints," *DSN Prog. Rep.*, vol. 42, no. 56, 1980.
- [25] J. Hamkins and B. Moision, "Multipulse pulse-position modulation on discrete memoryless channels," *The Interplanetary Netw. Prog. Rep.*, vol. 42, no. 161, pp. 1–13, 2005.
- [26] M. K. Simon and V. A. Vilmrotter, "Performance analysis and tradeoffs for dual-pulse PPM on optical communication channels with direct detection," *IEEE Trans. Commun.*, vol. 52, no. 11, pp. 1969–1979, 2004.